



## Study on the effectiveness of spent waste sugarcane bagasse for adsorption of different petroleum hydrocarbons water pollutants: kinetic and equilibrium isotherm

Nour Sh. El-Gendy\*, Hussein N. Nassar

*Petroleum Biotechnology Lab., Process Development Department, Egyptian Petroleum Research Institute, Nasr City, Cairo 11727, Egypt, Tel. +20 1001443208; email: nourepri@yahoo.com (N.Sh. El-Gendy), Tel. +20 1220600822; email: hessen\_nasar@hotmail.com (H.N. Nassar)*

Received 5 July 2014; Accepted 30 December 2014

---

### ABSTRACT

This study investigates the capability of spent waste sugarcane bagasse (SWSB), obtained from bioethanol production process, for biosorption of diesel oil and kerosene, in an attempt to be applied for wastewater treatment with an enrichment of the SWSB for its use as a renewable solid biofuel. The chemical composition, microstructure, surface morphology, and reactive surface functionalities of the adsorbent were determined. Effect of different pH, salinity, initial pollutant concentrations, temperatures, and adsorbent dosages were also studied. The results showed that the sorption of petroleum products depends on the adsorbent material and the adsorbate type. The biosorption was favorable, where the SWSB removed 63–41% of diesel oil and 70–50% of kerosene in solutions containing 5–20% w/v of these contaminants. The kinetic equilibrium was reached after 6 h and the biosorption follows the pseudo-second-order rate expression. The SWSB expressed good biosorption capacity 44–86 and 78–110 mg/g over a wide range of pH and salinities. The biosorption potential increased with increase in the temperature and decreased with increase in the biosorbent dosage. The sorption may be partly due to absorption/partitioning of pollutants onto the SWSB and partly due to adsorption onto the surface of SWSB. The linear, Freundlich, and Temkin models could provide adequate fit for sorption onto the SWSB, while Langmuir model provided the best adequate fit at low temperature. The analysis of the obtained isotherm data proved the predominance of chemisorption and the endothermic nature of the biosorption process. The calorific value of the SWSB recorded  $\approx 32.91$  and 33.61 MJ/kg for SWSB after biosorption of diesel oil and kerosene, respectively. The results recommend the applicability of the low cost, readily available, sustainable and environmentally friendly SWSB for wastewater treatment, and production of a renewable solid biofuel, which would have positive impact on economy, energy, and environment.

*Keywords:* Clean-up; Water pollution; Spent waste sugarcane bagasse; Biosorption mechanism; Solid biofuel

---

\*Corresponding author.

## 1. Introduction

Water pollution is a vital problem and appropriate planning and necessary acts should be done to avoid and reduce this pollution. One of the main sources of water contamination is oil spills or oily wastewaters. Petroleum oil and its products pollute all water streams such as seas, oceans, rivers, or underground waters. Oil spills may be due to the discharge of crude oil or its derived products such as gasoline, kerosene, diesel, or machine oil from tankers, ships, offshore platforms, heavier fuels used by large ships, accidents in pipelines, or production process, as well as spills of other oily wastewaters such as produced water, drilling mud, cuttings, refineries effluents, and ballast water [1,2].

There are many different ways that oil spills can be cleaned-up: mechanical, chemical, and biological methods. The methods chosen to clean-up an oil spill are determined based upon the type of the spilled oil, the location and its proximity to sensitive environments, and other environmental factors. Mechanical methods include booms, skimmers, and truck vacuums. Chemical methods include dispersants, surface washing agents, and surface collecting agents. While, biological methods include the use of microbiological cultures, enzyme additives, and nutrient additives to increase the rate of biodegradation of the contaminants [3,4]. However, there are many limitations for those treatments such as low efficiency, high operation cost, corrosion, and recontamination [2]. Sorption on spill-clean-up sorbents is the most safe and effective processes used for treating oil spills. The spill-clean-up sorbents have oil sorption capacity ranging from 0.26 to 86 g/g, depending on the type of the sorbent and on the type and the initial concentration of the spilled oil [5]. Organic sorbents derived from plants, such as sea plants, cotton fibers, saw dust, corncob, coconut fibers, sugarcane bagasse, rice straw, and barley straw, are often preferred over inorganic and synthetic sorbents, since they are more readily available, cheap, biodegradable, and typically have higher oil sorption capacity [2,6,7].

Agricultural crops wastes in Egypt have been estimated to amount range from 30 to 35 million tons/year, with 8.7 million tons/year sugarcane residues, including 4.7 million tons/year sugarcane bagasse, which adds to environmental pollution [8]. The application of this waste in wastewater treatment would offer a triple-fact solution: economic, environmental, and waste management. Modified sugarcane bagasse has been reported as efficient adsorbent for different water pollutants including heavy metals, phenols, and dyes [9–11]. But, the pre-treatment adds to the cost of

the process. Brandao et al. [6] reported the good efficiency of untreated sugarcane bagasse for adsorption of gasoline and n-heptane from aqueous solution.

The aim of this study is to investigate the capacity of untreated spent waste sugarcane bagasse (SWSB), obtained from bioethanol fermentation process, for adsorption of different petroleum hydrocarbons products in a batch process. The physicochemical characterization of the adsorbent was done to understand the adsorption process. The effects of different parameters: pH and salinity of solution, initial adsorbate concentration, time, temperature, and adsorbent dosage were studied. The kinetics of the adsorption was also studied to provide information about the mechanism of adsorption, which is important for the efficiency of the process. Different isotherm models were applied to describe the interactive behavior between the adsorbate and adsorbent, which is important for investigating mechanism of adsorption. Analysis of equilibrium data was also done to develop an equation that accurately represents the results and could be used for design purposes. The calorific value of the adsorbate after adsorption process was evaluated in an attempt to be used as solid biofuel.

## 2. Materials and methods

### 2.1. Biosorbent

SWSB was used as the biosorbent in this study. It is a spent waste biomass, obtained after its solid state fermentation using *Trichoderma viride* F-94 and *Aspergillus niger* F-98 for bioethanol production, which is undertaken in the Petroleum Biotechnology Laboratory of the Egyptian Petroleum Research Institute. The collected biomaterial was washed with hot deionized water, dried in a hot air oven at 105°C until a constant weight, crushed with grinder, sieved to constant sizes (0.25–0.315 mm), and then used as it is without any further chemical or physical treatments.

Cellulose, hemicellulose, and lignin percentages in SWSB were determined in the Agricultural Research Center, Giza, Egypt.

Fourier transform infrared (FTIR) spectra in the wavenumber 4,000 to 400  $\text{cm}^{-1}$  range were recorded for the SWSB before and after biosorption process, in the form of tablets pressed with KBr, using Perkin-Elmer model spectrum one FTIR spectrometer (CA, USA).

The microstructure and surface morphology of the biosorbent were characterized by JEOL model JSM-53000 scanning electron microscope (SEM, Jeol, Tokyo, Japan) with an accelerating voltage 20 kV at various magnifications.

## 2.2. Adsorbate

Two petroleum products were used in this study: kerosene and diesel oil with viscosity 2.2 and 3.3 cSt and density 0.78701 and 0.85204 g/cm<sup>3</sup>, respectively. The hydrocarbon skeleton of these adsorbates was determined by gas chromatography (Agilent model 6890, CA, USA) equipped with a flame ionization detector GC-FID, according to the method reported by Amer et al. [12].

## 2.3. Batch adsorption studies

The batch biosorption experiments were conducted by contacting 50 mL of known adsorbate (kerosene or diesel oil) concentration with certain amount of the dried biomass (SWSB) as the adsorbent in 250 mL Erlenmeyer flasks closed with parafilm "M" to prevent evaporative loss and placed in a rotary shaking incubator of 150 rpm, set at different temperatures (Table 1). The biosorbent was separated from the solution at predetermined time intervals by centrifugation at 2,000 rpm for 10 min. The residual adsorbate concentration in the supernatant solution was separated through decantation and then weighed. The separated aqueous phase was also subjected to extraction by carbon tetrachloride (1:1 v:v), to determine gravimetrically the concentration of any hydrocarbons left in the aqueous phase [13]. Then the total weight of nonadsorbed pollutant was determined. The biosorbent before and after each adsorption experiment was dried overnight at 60°C and then weighed to calculate the exact quantity of the pollutant removal.

Negative controls (NC) were carried out according to the required experimental conditions (Table 1); NC1 (with different adsorbates but without biosorbent) to

ensure that, the sorption is by the dried biomass only and any sorption effect of hydrocarbons onto the wall of the flasks is negligible; and NC2 (with biosorbent but without any adsorbate) to eliminate any discrepancies that might be caused by adsorption of water.

The adsorption capacity and the percentage of pollutant removal were determined at different pH, salinity, and contact time with different initial pollutant concentrations to know the equilibrium contact time, and study the kinetics of the biosorption process. The biosorption isotherm at different temperatures was also studied using different biosorbent concentrations. The pH of the solution was adjusted using 0.1 M HCl or 10% NaOH. Table 1 summarizes all the process factors used for adsorption experiments. All the experiments were carried out in triplicates and the listed data are average of the obtained results.

The removal percentage and the biosorption capacity  $q_t$  mg/g were calculated as follows, respectively:

$$\text{Removal \%} = \frac{(C_0 - C_t)}{C_0} \times 100 \quad (1)$$

$$q_t = \frac{(C_0 - C_t)V}{M} \quad (2)$$

where  $C_0$  and  $C_t$  are the initial and final pollutant concentrations (mg/L), respectively,  $V$  (L) is the volume of the solution, and  $M$  (g) is the mass of the biosorbent.

## 2.4. Evaluation of gross calorific value

The gross calorific value of the SWSB before and after biosorption process was evaluated according to

Table 1

Experimental conditions used for biosorption of different petroleum hydrocarbon pollutants by spent waste sugarcane bagasse SWSB

Process factors	Other conditions
Solution pH Different pH 3–9	Contact time 24 h, temperature 303 K, agitation speed 150 rpm, adsorbent dosage 4% (w/v), pollutant concentration 15% (w/v), and salinity 10 g/L NaCl
Solution salinity Different NaCl concentration 0–40 g/L	Contact time 24 h, temperature 303 K, agitation speed 150 rpm, pH 3, adsorbent dosage 4% (w/v), and pollutant concentration 15% (w/v)
Contact time 1–24 h Different pollutant concentrations 5–20% (w/v)	Temperature 303 K, agitation speed 150 rpm, pH 3, adsorbent dosage 4% (w/v), and salinity 10 g/L NaCl
Isotherm studies at different temperatures 288, 303, and 318 K	Contact time 12 h, agitation 150 rpm, pH 3, salinity 10 g/L NaCl, pollutant concentration 15% (w/v), and different adsorbent dosage 1–8% (w/v)

the ASTM D2015-96 [14], by calorific value tester, Sanyo Gallenkamp, PLC, England.

### 3. Results and discussion

#### 3.1. Characterization of SWSB

The polysaccharide-based biosorbent SWSB is composed of 17% cellulose, 18% hemicellulose, and 8% lignin and the rest are ashes containing minor and trace elements.

The chemical structure of biosorbent is of vital importance in understanding the adsorption process. FTIR spectrum in Fig. 1 identifies the characteristic functional groups in the biosorbent which are accountable in the biosorption process. The broad and intense peak around  $3,361\text{ cm}^{-1}$  corresponds to the stretching vibration of hydrogen bonded hydroxyl

groups of cellulose and lignin. The peak around  $1,632\text{ cm}^{-1}$  of  $-\text{OH}$  together with  $\text{C}=\text{C}$  in the aromatic rings indicates the presence of plenty of polyphenols [15]. The peaks at  $2,920$ ,  $1,458$ , and  $1,375\text{ cm}^{-1}$  are assigned mainly to  $\text{CH}_2$  units in biopolymers [16]. The peak around  $1,735\text{ cm}^{-1}$  is assigned for carbonyl,  $\text{C}=\text{O}$  of polysaccharides [17]. The peak around  $1,514\text{ cm}^{-1}$  represents the  $\text{C}=\text{C}$  rings stretching vibration of lignin [18]. The peaks around  $1,250$  and  $1,108\text{ cm}^{-1}$  are due to the  $\text{C}-\text{O}$  stretching of polysaccharides [18]. Peak at  $608\text{ cm}^{-1}$  can be attributed to the aromatic  $\text{C}-\text{H}$  components [19].

In conclusion, it can be well indicated that the hydroxyl and carboxyl groups are present in abundance. According to Srivastava et al. [20], the presence of polar groups on the surface is likely to provide considerable cation exchange capacity to the adsorbents. Rocha et al. [21] reported that the presence of lignin in

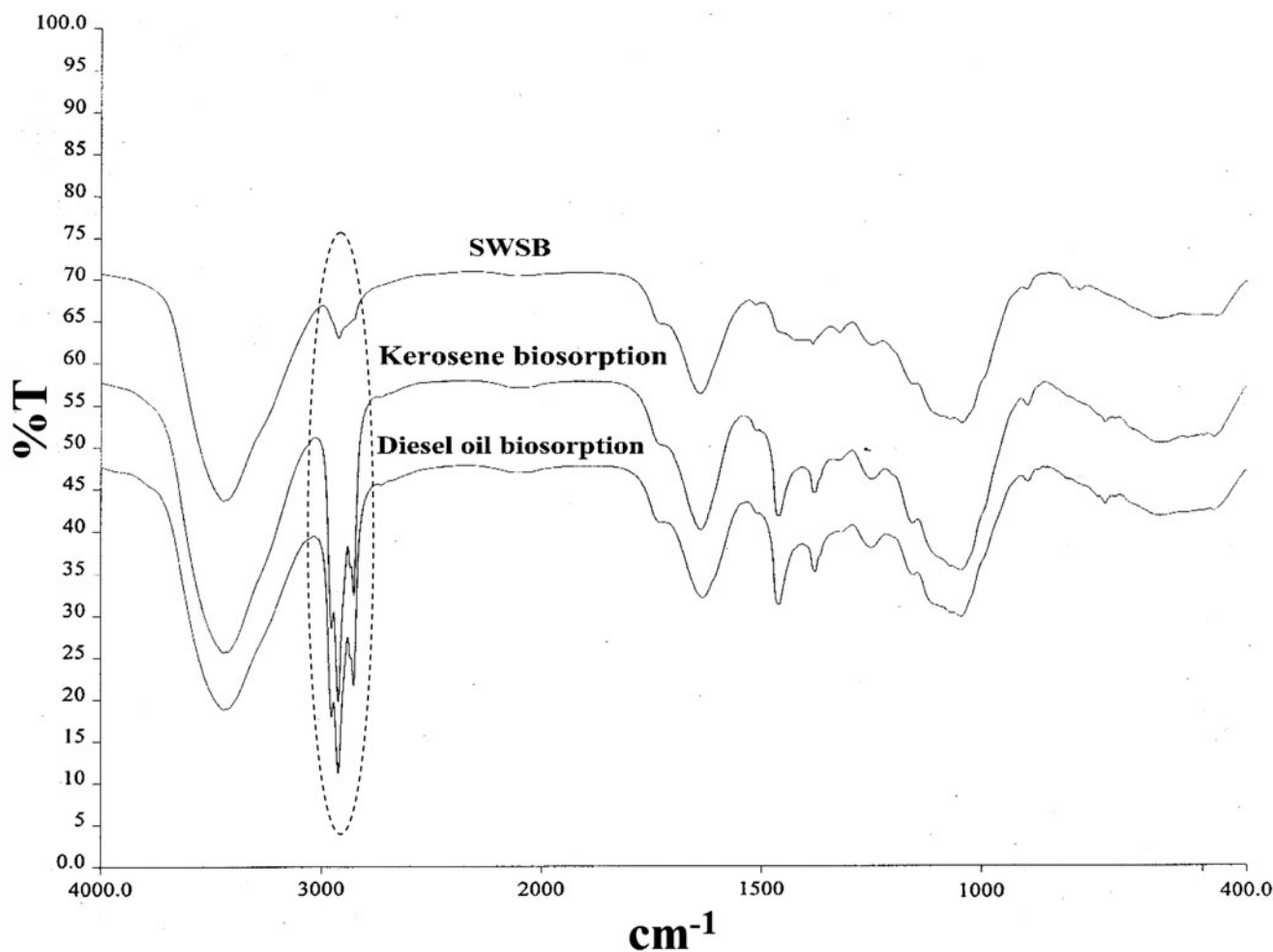


Fig. 1. FTIR spectra of spent waste sugarcane bagasse SWSB before and after biosorption of different petroleum hydrocarbons pollutants.

bagasse which is built-up from phenyl propane nucleus; an aromatic ring with a three carbon side chain is promptly an effective constituent to adsorb organic molecules and polyaromatic hydrocarbons PAHs. Wang et al. [22] reported that the polyaromatic frame is highly effective for adsorption. Crisafulli et al. [23] reported that the natural polymer lignin fraction has been identified as the principal factor determining the degree of sorption of nonpolar compounds.

The asymmetric and symmetric stretching vibration of methylene C–H adsorption bands were found to be much stronger after the biosorption of kerosene and diesel oil (Fig. 1), suggesting adsorption of these petroleum hydrocarbon pollutants to hydrophobic groups, i.e. the alkyl chain layer of the SWSB surface. Similar observation was reported by Ibrahim et al. [2], for biosorption of emulsified oil from oily wastewater onto barley straw and was also reported by Kenes et al. [7], for biosorption of petroleum onto thermally treated rice husks.

The SEM pictures of SWSB at different magnifications (Fig. 2) show the irregular shape, high surface area (Fig. 2(a)), and porous structure of the adsorbent with round holes on the surface (Fig. 2(c)). The presence of channels and different pore sizes could be also observed (Fig. 2(b) and (c)). Wang et al. [22] reported that the high surface area and porous structure are requested for an effective adsorbent. Brandao et al. [6] reported that the highly hydrophobic characteristic of biomass combined with its large surface area and high porosity develop a capillary force toward the adsorption of oils, and tend to adsorb organic contaminants

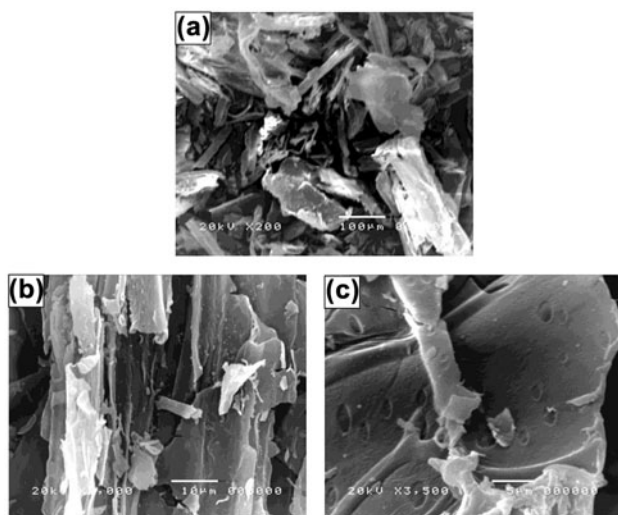


Fig. 2. SEM pictures of SWSB.

through physical and chemical mechanisms. Kenes et al. [7] reported that the high petroleum sorption ability is determined by the porous structure of the adsorbents, as well as by the physical and chemical interactions of their functional groups with the crude oil components.

### 3.2. Effect of pH

The solution pH is an important parameter in the adsorption process as it influences the adsorbent surface properties and its binding sites [24]. The effect of pH on biosorption of the studied different petroleum hydrocarbon fractions kerosene and diesel oil is illustrated in Fig. 3. The biosorption activity decreases as the pH increases, recording 110 and 86 mg/g at pH 3, respectively. It decreased to 98 mg/g at pH 5 and remained nearly sustained at higher pH values, recording 95 mg/g in the case of biosorption of kerosene. But in the case of diesel oil, biosorption decreased to 56 mg/g at pH 5 then further decrease occurred at pH 7, recording 49 mg/g and remained nearly sustained at higher pH, recording 44 mg/g at pH 9. The decrease of adsorption capacity at high pH value was also reported by Ibrahim et al. [2]. Hydrocarbon and oil droplets often carry negative charge in aqueous solution [25]. Thus, negative charge on the biosorbent surface at high pH may hinder sorption through electrostatic repulsion and this may have an adverse impact on the biosorption processes.

In this study, the pH dependence was lower for sorption of kerosene than that of diesel oil on the SWSB, where the biosorption capacity decreased by  $\approx$  15 and 42 mg/g with the pH increment from pH 3 to pH 9 in case of kerosene and diesel oil, respectively. This phenomenon was also observed by Mishra and Mukherji [5] for biosorption of diesel and lubricating

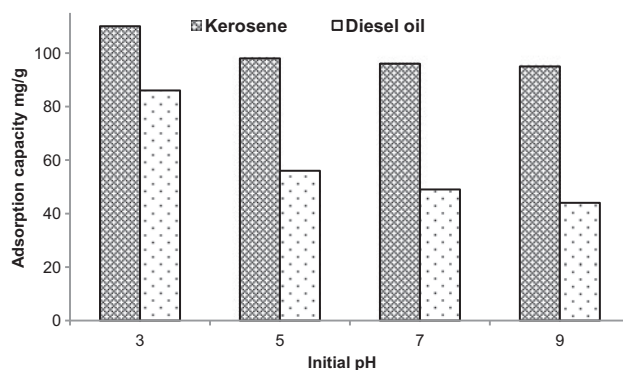


Fig. 3. Effect of solution pH on hydrocarbon uptake onto spent waste sugarcane bagasse.

oil on algal biomass, the pH dependence was lower for sorption of diesel than for sorption of lubricating oil. According to Weber and Digiano [26], sorption of oil on biosorbent may be partly due to absorption/partitioning of oil onto the organic matter and partly due to the adsorption onto the surface of the biosorbent due to some specific interactions. Absorption/

partitioning of hydrocarbons is expected to be a faster phenomenon compared to adsorption. The absorption can be explained by linear isotherms while the adsorption is manifested in terms of nonlinear sorption isotherms. The impact of pH on absorption/partitioning may be negligible but pH may have a strong influence on the adsorption. It is difficult to determine the

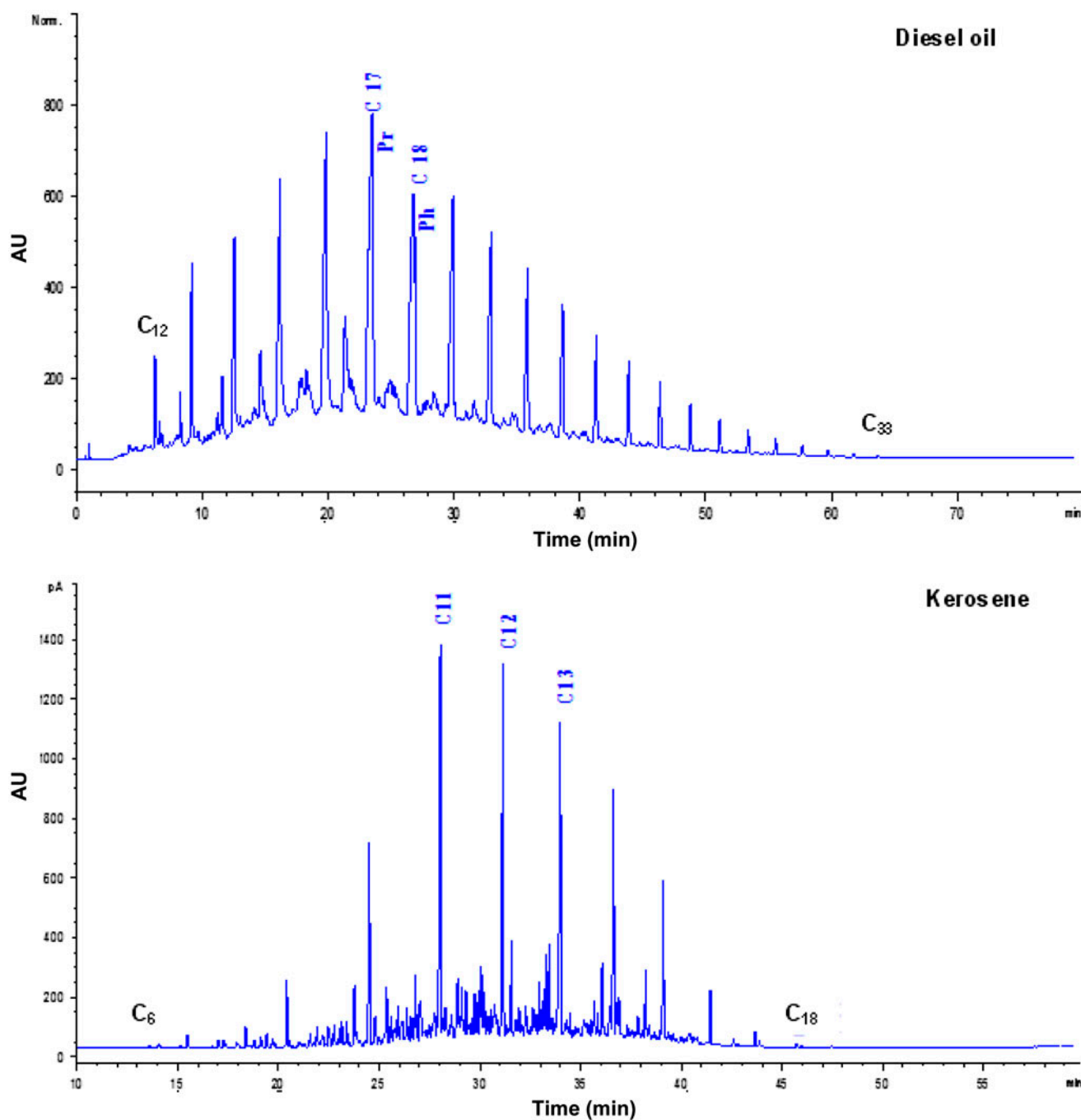


Fig. 4. Hydrocarbon skeletons of the adsorbates.

relative contribution of the two processes for complex adsorbates such as kerosene and diesel. But from the listed results, it is possible to conclude that, the contribution of absorption/partitioning is more for sorption of kerosene on the SWSB compared to that of diesel oil. This might be attributed to the viscosity, density, and hydrocarbon components of the pollutant itself. Kerosene is characterized by lower viscosity and density than that of diesel oil, where its hydrocarbon skeleton ranged between  $nC_6$  and  $nC_{18}$ , which superimposed on smaller unresolved complex mixture UCM hump (naphthenes, cycloalkanes, and aromatics) compared to that of diesel oil, which composed of hydrocarbon skeleton ranged between  $nC_{12}$  and  $nC_{33}$  superimposed on a larger UCM hump (Fig. 4).

### 3.3. Effect of salinity

It is important to study the effect of the salinity of the solution, for the application of this biosorbent in real field applications, i.e. for biotreatment of different polluted aqueous environment with different salinities. It is obvious from Fig. 5 that the effect of salinity on biosorption of kerosene is higher than that of diesel oil, where the biosorption of kerosene increased from 83.86 to 108.52 with the increase of the salinity to 10 g/L NaCl then decreased with further increment of the salinity, recording; 77.53 mg/g at salinity of 40 g/L NaCl. While, the biosorption of diesel oil slightly increased from 81.36 to 85.57 mg/g with the increase of the salinity to 10 g/L NaCl then slightly decreased with further increment of the salinity, recording; 75.95 mg/g at salinity of 40 g/L NaCl. Thus, it can be concluded from this study that the SWSB can be applied for biotreatment of different types of polluted water streams over a wide range of salinity.

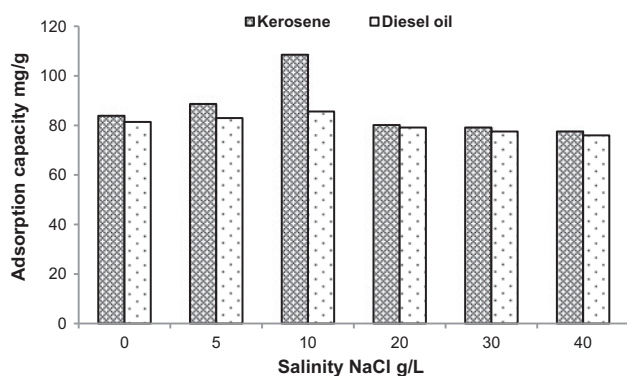


Fig. 5. Effect of solution salinity on hydrocarbon uptake onto spent waste sugarcane bagasse.

### 3.4. Effect of initial pollutant concentration and contact time

Biosorption of kerosene and diesel oil at different concentrations (5, 10, 15, and 20% w/v) onto the SWSB was studied as a function of contact time (Figs. 6 and 7). Generally, the biosorption of kerosene was higher than that of diesel oil at all the studied concentration range, this might be attributed to the lower viscosity and density of kerosene than that of diesel oil, which would make the diffusion rate of the kerosene across the external boundary layer toward the adsorbent particles, higher than that of diesel oil. These results confirm that sorption of petroleum hydrocarbon fractions depends on both the adsorbent material and the adsorbate type. It can be seen from Figs. 6 and 7 that the biosorption increases with time, till equilibrium is attained, nearly after 6 h, therefore, equilibrium time was set conservatively at 12 h. The adsorption curves are smooth and continuous leading to saturation at various pollutant concentrations on the outer interface of the biomass. This shows the possibility of monolayer coverage of pollutant onto the outer interface of the dried biomass

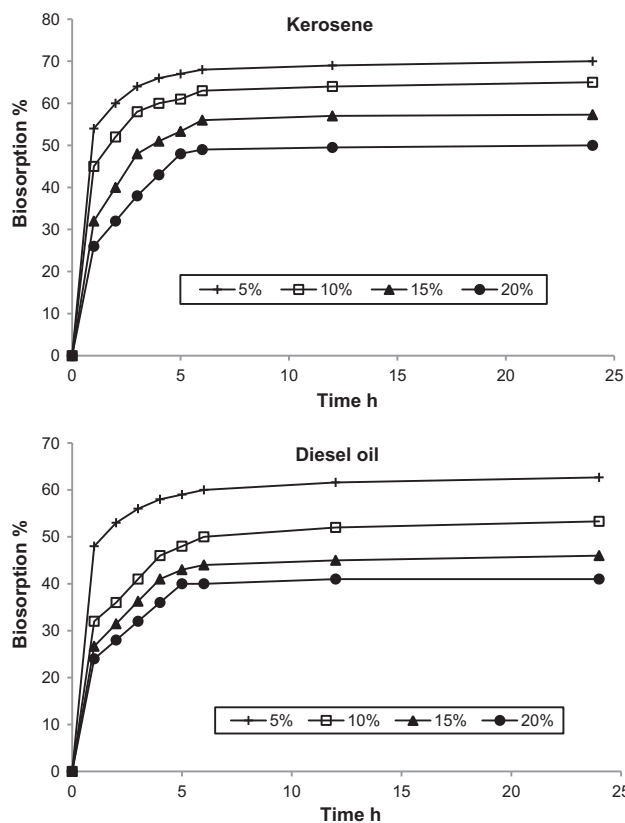


Fig. 6. Effect of contact time at different initial pollutant concentration on its percentage removal by spent waste sugarcane bagasse.

[27]. The biosorption was found to be initially rapid, recording percentage removal of  $\approx 54, 45, 32,$  and  $26\%$ ,  $48, 32, 27,$  and  $24\%$  of  $5, 10, 15,$  and  $20\%$  w/v initial concentration of kerosene and diesel oil within the first 1 h, respectively. Then the pollutant removal tends to proceed in slower rate until reaching equilibrium, recording  $\approx 68, 63, 56,$  and  $49\%$ ,  $60, 50, 44,$  and  $40\%$  after 6 h, respectively (Fig. 6). Similar observation was reported by Kenes et al. [7] for the biosorption of petroleum on thermally treated rice husks, and explained this as, at first the adsorbent absorbed petroleum by macropores and afterward it penetrated into the micropores until reaching equilibrium time. This was also observed by Ibrahim et al. [2] through removal of emulsified oil using barely straw, and attributes the initial high rate uptake to the existence of bare surface. Initially, large number of vacant surface sites is available for adsorption, thus, there would exist an increased concentration gradient between adsorbate in solution and adsorbate on the adsorbent. So, the adsorption rate is very fast thus increases rapidly the amount of pollutant (adsorbate) accumulated onto SWSB surface approximately

within the first 1 h of adsorption process. As a result, the remaining vacant surface sites are difficult to be occupied due to formation of repulsive forces between the pollutant molecules on the solid surface and the bulk phase. Pollutant molecules have to penetrate deeper into pores encountering much higher resistance. This might explain the decrease of adsorption rates, as less adsorption sites are available. Similar observation was also reported by Brandao et al. [6] for biosorption of gasoline and n-heptane onto sugarcane bagasse.

In this study, the percentage of pollutant removal decreases with increase in its initial concentration (Fig. 6). This may be due to the saturation of the sorption sites on the biosorbent as the concentration of pollutant increases. But the actual amounts of pollutant adsorbed increase with the increase of its initial concentration (Fig. 7), recording  $\approx 43, 79, 105,$  and  $123$  mg/g,  $38, 63, 83,$  and  $100$  mg/g after 6 h for the initial pollutant concentration of  $5, 10, 15,$  and  $20\%$  w/v, in case of kerosene and diesel oil, respectively. This means that the increase in adsorption is limited with biosorbent dose. According to Mane et al. [28], this phenomenon might be due to the increase in the driving force of the concentration gradient with the initial adsorbate concentration. That would increase the mass transfer of pollutant molecules from the solution onto the biosorbent surface. Hence, a higher initial pollutant concentration enhances the adsorption process and as the adsorption process precedes the driving force decreases with time.

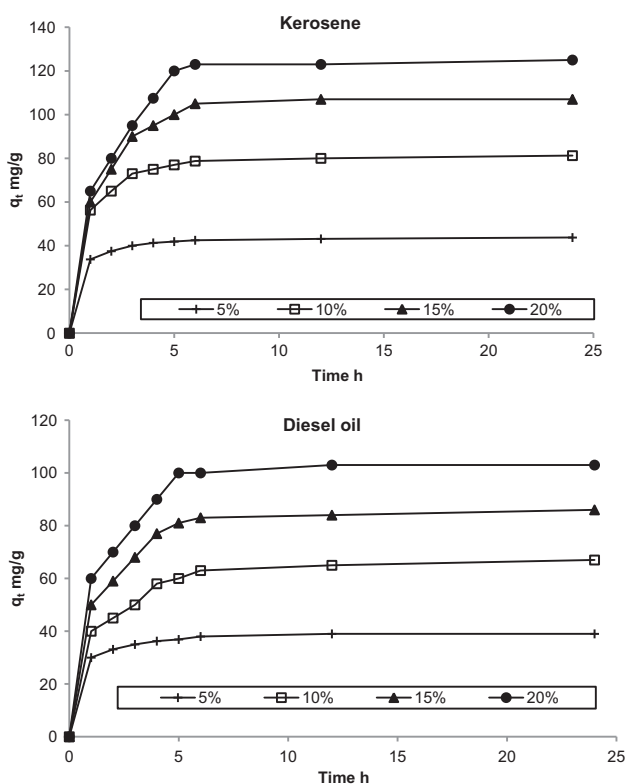


Fig. 7. Effect of contact time at different initial pollutant concentration on its actual uptake (mg/g) by spent waste sugarcane bagasse.

### 3.5. Biosorption kinetic modeling

In order to investigate the biosorption process of kerosene and diesel oil onto the SWSB, two kinetic models (Table 2) were tested for the obtained data to elucidate the biosorption mechanism. The best fit model was selected based on the linear regression correlation coefficient,  $R^2$  values. It can be noticed that the theoretical  $q_{e,cal}$  mg/g values calculated from pseudo-second-order model equation are the closest to the experimental  $q_{e,exp}$  mg/g values. Fig. 8 illustrates the linear plots of the pseudo-second-order model equation for biosorption of pollutants onto SWSB. Based on the highest value of  $R^2$  listed in Table 2, it was found that the biosorption process follows the pseudo-second-order rate expression. This suggests that the overall rate of the kerosene and diesel oil biosorption process onto the SWSB appears to be controlled by chemisorption process or combination of both physical and chemical sorption process [30]. It can also be seen in Table 2 that with an increase in initial pollutant concentration, the equilibrium sorption

Table 2

Pseudo-first- and second-order kinetic models for biosorption of different pollutant concentrations onto SWSB

Kinetic models	Kerosene				Diesel oil			
	5%	10%	15%	20%	5%	10%	15%	20%
Pseudo-first-order kinetic Lagergren [29]								
$\log(q_e - q_t) = \log q_e - \frac{K_1}{2.303} t$ (3)								
$R^2$	0.789	0.8328	0.786	0.9698	0.9234	0.9716	0.9890	0.9469
$K_1$ (h <sup>-1</sup> )	0.314	0.324	0.372	0.598	0.430	0.523	0.540	0.602
$q_{e,calc}$ (mg/g)	13.57	31.52	72.58	103.73	22.39	54.53	77.64	105.10
Pseudo-second-order kinetic Ho and McKay [30]								
$\frac{t}{R^2} = \frac{1}{K_2 q_e^2} + \frac{1}{q_e} t$ (4)								
$R^2$	1	0.9999	0.9992	0.9982	0.9999	0.9994	0.9993	0.9987
$K_2$ (g/mg h)	0.073	0.029	0.014	0.009	0.073	0.016	0.015	0.013
$q_{e,calc}$ (mg/g)	44.25	82.64	111.11	129.87	39.68	69.44	89.29	107.53
$h_0$ (mg/g h)	142.86	196.08	166.67	153.85	114.94	79.37	123.46	149.25

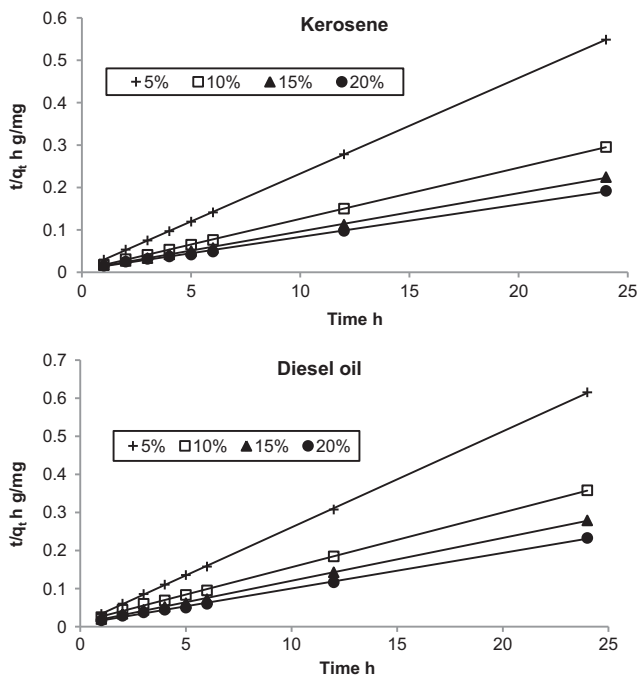


Fig. 8. Pseudo-second-order kinetic plots for biosorption of different pollutant onto spent waste sugarcane bagasse.

capacity increased and the rate constant of adsorption  $K_2$  (g/mg h) decreased. But the initial adsorption rate  $h_0$  (mg/g h) did not follow a certain trend. This might confirm that the sorption of oil on biosorbent may be partly due to absorption/partitioning of oil onto the organic matter and partly due to the adsorption onto the surface of the biosorbent due to some specific interactions.

### 3.6. Effect of temperature on the biosorption process

Increasing the temperature increased the biosorption capacity of the SWSB (Fig. 9). This indicates an endothermic system and the creation of some new active sites, with increase in temperature for additional adsorption on the surface of the sorbent is also endothermic [24]. This also confirms a chemisorption mechanism, where there is an increase in the number of molecules acquiring sufficient energy to undergo chemical reaction with increasing temperature. According to Gupta et al. [31], increasing the temperature decreases the viscosity of the solution, which consequently would increase the diffusion rate of the adsorbate molecules across the external boundary layer toward the adsorbent particles and the internal pores of the adsorbent particles. Similar observation was reported by Ibrahim et al. [2] for biosorption of emulsified oil from oily wastewater onto barely straw, and explained this by the increment of the movement of adsorbate molecules with elevated temperatures which would increase the interaction between sorbent and adsorbate molecules, thus increase the diffusion rate of the adsorbate molecules across the adsorbent surface. The increase in temperature from 288 to 313 K may have increased the diffusivity of oil and thus overcome mass transfer rate limitation [32]. Thus, low sorption at 288 K may be attributed to rate limited mass transfer. The enhancement of the adsorption capacity of the adsorbent at high temperatures may be also attributed to the enlargement of pore size and activation of the adsorbent surface [24].

### 3.7. Effect of biosorbent dosage

Within all the studied range of temperatures 288–318 K, as the biosorbent dosage increased the

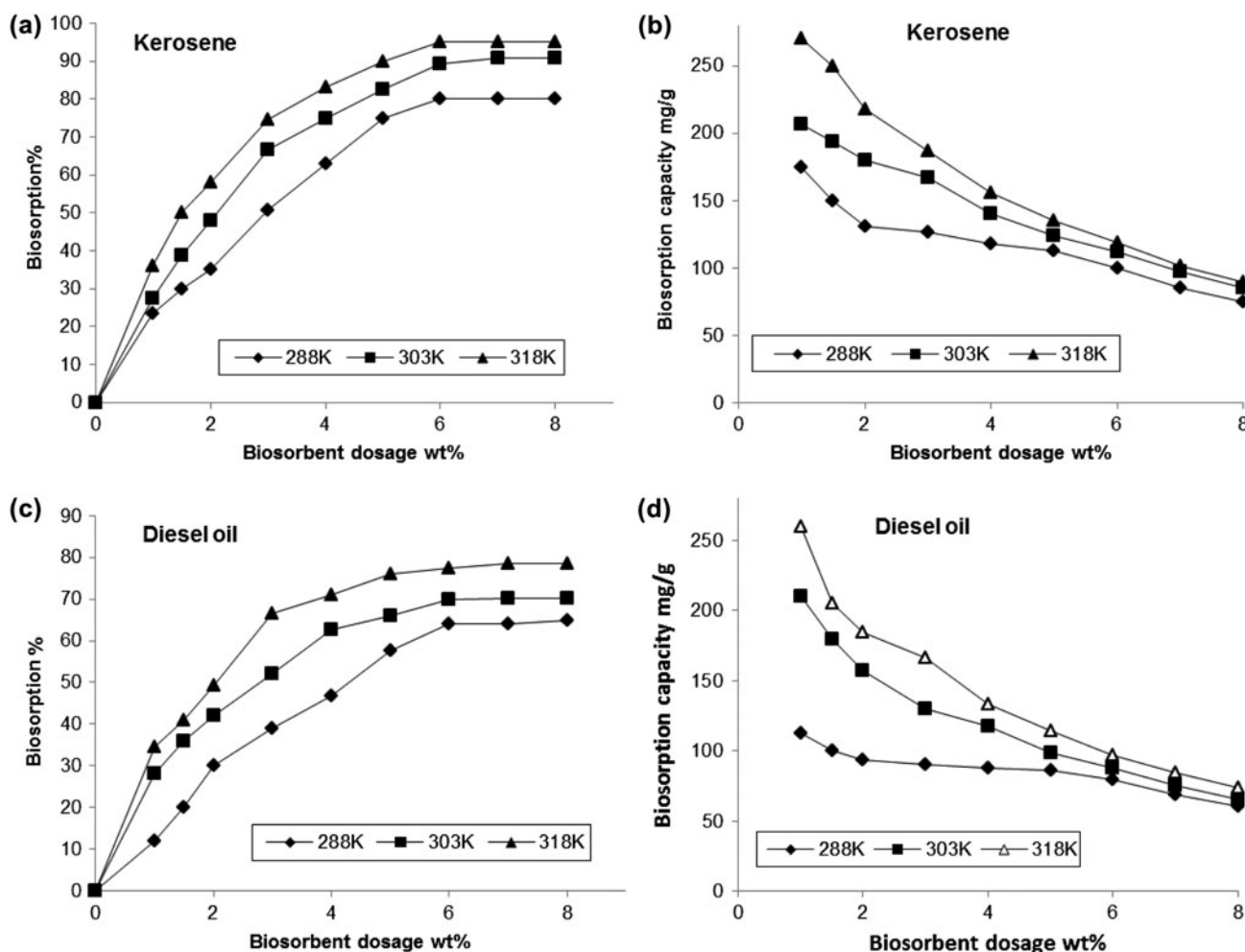


Fig. 9. Effect of temperature and biosorbent dosage on biosorption process.

biosorption efficiency increased (Fig. 9(a) and (c)), however, the biosorption capacity  $q_e$  (mg/g) decreased (Fig. 9(b) and (d)). Similar observation was reported by Ibrahim et al. [2], for biosorption of emulsified oil from oily wastewater onto barely straw and attributed the increase of adsorption efficiency to the more available binding sites, due to the increase of surface area, while, the decrease in adsorption capacity was due to the higher unsaturated adsorption sites. According to Bohel et al. [34], the presence of relatively higher concentration of biosorbent in the solution resulting in reduced distances between the biosorbent particles, thus making many binding sites unoccupied. According to Iscen et al. [35], the interparticles interactions such as aggregation, overlapping, and overcrowding occur at high biosorbent concentration and also lead to unoccupied binding sites. Malik [36] mentioned another possible explanation, the splitting effect of concentration gradient between the adsorbate

molecules and biomass (biosorbent) concentration causes a decrease in the amount of pollutant biosorption onto unit weight of biomass.

### 3.8. Biosorption isotherm

The analysis of the obtained equilibrium data is important to develop an equation which would accurately represent the results and could be used for design purposes.

The practically linear isotherms, as illustrated in Fig. 10, with correlation coefficient:  $0.8684 \leq R^2 \leq 0.9766$  and  $0.8238 \leq R^2 \leq 0.9768$  for kerosene and diesel oil, respectively, may indicate that the sorption of pollutant on the biosorbent may be partly due to absorption/partitioning of the pollutant onto organic matter and partly due to the adsorption onto the surface of the biosorbent due to some specific interactions. Similar phenomenon was reported by Chen et al. [37] for the biosorption of

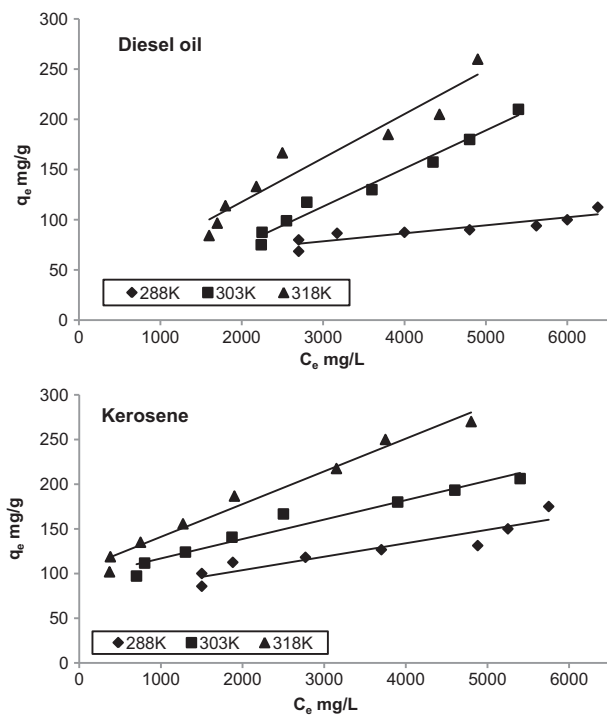


Fig. 10. Linear sorption isotherm of different pollutant onto SWSB.

persistent organic pollutants from aqueous solution using different plant residues. The partition coefficient  $K_d$  derived from the studied batch sorption experiments can be calculated from the equation:

$$K_d = \frac{q_e}{C_e} \quad (5)$$

Partition coefficient  $K_d$  is a good parameter to describe the distribution of organic pollutants between solid and solution phases, and then to evaluate the sorption capacity of the sorbents. It is obvious from data listed in Table 3 that  $K_d$  increased with the increase of temperature.

The Langmuir adsorption isotherm [38] is based on the assumption of monolayer adsorption on a structurally homogeneous adsorbent, where all the sorption sites are identical and energetically equivalent, and there are no interactions between the molecules adsorbed on neighboring sites. Characteristic constants of Langmuir equation  $K_L$  and  $a_L$  can be determined from the following linearized form:

$$\frac{C_e}{q_e} = \frac{1}{K_L} + \frac{a_L}{K_L} C_e \quad (6)$$

The theoretical maximum adsorption capacity ( $q_{e,max,theo}$ ) corresponding to Langmuir constants is numerically equal to  $K_L/a_L$  [39].

The essential features of Langmuir can be expressed in terms of dimensionless constant separation factor  $R_L$  which was defined by Weber and Chakravorti [40] as:

$$R_L = \frac{1}{1 + a_L C_o} \quad (7)$$

Values of  $R_L$  indicate the shapes of isotherms to be either unfavorable ( $R_L > 1$ ), linear ( $R_L = 1$ ), favorable ( $0 < R_L < 1$ ), or irreversible ( $R_L = 0$ ), where  $C_o$  (15% w/v) is the maximum initial pollutant concentration used in the isotherm studies. Langmuir constants  $a_L$  and  $K_L$  can be determined from the linear plots of  $C_e/q_e$  vs.  $C_e$  at different temperatures. All the isotherm data are listed in Table 3. The correlation coefficient of the kerosene biosorption ranged between  $0.8549 \leq R^2 \leq 0.9918$ , indicating monolayer coverage, while that of diesel oil at low temperature 288 K, recorded  $R^2$  0.9227 but at higher temperatures, recorded; 0.1535 and 0.5778 at 303 and 318 K, respectively. This indicates that biosorption of diesel oil onto SWSB at low temperatures obeying Langmuir isotherms with monolayer coverage, but at higher temperatures does not obey Langmuir isotherm. It can be observed that  $R_L$  at different temperatures ranged between  $0.085 \leq R_L \leq 0.175$  and  $0.172 \leq R_L \leq 0.860$  for kerosene and diesel oil, respectively, which confirms favorable isotherm. The lower the  $R_L$  value, the more favorable the isotherm is.

The Freundlich isotherm model [41] is an empirical expression which represents the multilayer adsorption on heterogeneous surfaces where there are interactions between the adsorbed molecules. Characteristic constants of Freundlich model  $K_f$  (L/g) and  $n$  were determined from the following logarithmic linearized form:

$$\log q_e = \frac{1}{n} \log C_e + \log K_f \quad (8)$$

When plotting  $\log q_e$  vs.  $\log C_e$ , straight lines were obtained with  $0.8379 \leq R^2 \leq 0.9841$  and  $0.7958 \leq R^2 \leq 0.9651$  for kerosene and diesel oil, respectively. The obtained exponent  $n$  (Table 3) indicates the favorability of the adsorbent/adsorbate system where values of  $n$  were  $>1$  for all studied temperatures range. According to Treybal [42]  $n > 1$  represents favorable adsorption. It can be noticed from data listed in Table 3 that, the biosorption isotherms at higher temperatures fit well with Freundlich equation, indicating that the dominant mechanism is partition process [37].

Table 3  
Regression parameters of biosorption isotherms of kerosene and diesel oil onto spent waste sugarcane bagasse SWSB

Temperature	Parameters				
	$K_d$ (L/g)	Correlation coefficient			
<i>Linear equation</i>					
	Kerosene				
288K	0.0151	0.8684			
303K	0.0217	0.9521			
318K	0.0366	0.9766			
	Diesel oil				
288K	0.008	0.8238			
303K	0.0379	0.9768			
318K	0.0437	0.9259			
	$K_L$ (L/g)	$a_L$ (L/mg)	$q_{max, theo}$ (mg/g)	$R_L$	Correlation coefficient
<i>Langmuir model</i>					
	Kerosene				
288 K	0.100	$4.7 \times 10^{-4}$	212.77	0.175	0.8549
303K	0.212	$8.692 \times 10^{-4}$	243.90	0.103	0.9918
318K	0.327	$1.079 \times 10^{-3}$	303.03	0.085	0.9737
	Diesel oil				
288K	0.066	$4.8 \times 10^{-4}$	136.99	0.172	0.9227
303K	0.0407	$1.63 \times 10^{-4}$	250	0.860	0.1535
318K	0.0736	$1.03 \times 10^{-4}$	714.29	0.493	0.5778
	$K_f$ (L/g)		$n$		Correlation coefficient
<i>Freundlich model</i>					
	Kerosene				
288K	9.326		3.05		0.8379
303K	10.50		2.89		0.9841
318K	13.59		2.87		0.9785
	Diesel oil				
288K	4.91		3.33		0.7958
303K	7.44		1.04		0.9651
318K	28.31		1.2		0.9273
	$K_t$ (L/mg)	$B$	$b$ (J/mol)		Correlation coefficient
<i>Temkin model</i>					
	Kerosene				
288K	$6.69 \times 10^{-3}$	42.17	56.78		0.7798
303K	$9.86 \times 10^{-3}$	50.59	49.82		0.9828
318K	0.014	60.00	43.37		0.9507
	Diesel oil				
288K	$2.39 \times 10^{-3}$	38.43	62.31		0.813
303K	0.156	133.8	18.83		0.962
318K	0.174	137.07	18.99		0.9385

Temkin and Pyzhev [43] considered the effect of some indirect sorbate/adsorbate interactions on the adsorption isotherm. This isotherm assumes that the heat of adsorption of all the molecules in a layer decreases linearly with surface coverage of

adsorbent due to sorbate/adsorbate interactions [44]. This adsorption is characterized by a uniform distribution of binding energies. The Temkin isotherm can be represented by the following linear form:

$$q_e = B \ln K_t + B \ln C_e \quad (9)$$

where  $B = RT/b$ ,  $T$  is the absolute temperature in K,  $R$  is the universal gas constant (8.314 J/mol K), and  $K_t$  is the equilibrium binding constant. By plotting  $q_e$  vs.  $\ln C_e$ , straight lines were obtained with  $0.7798 \leq R^2 \leq 0.9828$  and  $0.813 \leq R^2 \leq 0.962$  for Kerosene and diesel oil, respectively (Table 3). Constant  $B$  which is related to the heat of adsorption increases with the increase in temperature, proving an endothermic adsorption. The values of  $b$  are greater than 8 J/mol indicating a strong interaction between pollutant molecules and biomass and chemisorption of an adsorbate onto the adsorbent [45–47].

The increase of  $K_d$ ,  $K_L$ ,  $K_t$ , and  $K_t$  with temperature indicates an increasing affinity of SWSB for kerosene and diesel oil with increasing temperature.

The shape of the isotherms (Fig. 9) is an example of a common behavior in physical adsorption with strong interaction forces between adsorbate and adsorbent. According to Brandao et al. [6], this is usually observed in the sorbents with a wide range of pore sizes distribution. The first part of the isotherm curves is characteristic with a favorable concave isotherm, such as a Langmuir isotherm, indicating monolayer coverage formation. According to Brandao et al. [6] this kind of shape is named class L, where large amounts of pollutant can be adsorbed at low concentrations of solute. This was also observed by the high percentage removal of kerosene and diesel oil in this region. After the monolayer formation, the adsorption takes place in multilayers, which is observed as inflections in the isotherm curves at higher pollutant concentrations. This can be confirmed by smaller inclination of the curve and the smaller percentages of adsorbed kerosene and diesel oil in the final range. Similar observation was reported by Brandao et al. [6] for biosorption of gasoline and n-heptane onto sugarcane bagasse, and attributed this to the decrease of the intensity of interaction forces between adsorbate and adsorbent at high concentrations of pollutants, due to the possibility that the solute molecules themselves may be clustered into micelles at higher pollutant concentrations making the adsorption process more difficult in some of the adsorbent pores by size exclusion.

By comparing results listed in Table 3, it is clear that, over all the studied range of temperatures, equilibrium data fit linear isotherm, Langmuir, Freundlich, and Temkin models, except, the biosorption of diesel oil onto SWSB, at high temperatures, does not follow Langmuir, expressing lowest  $R^2$ . This can be based on the fact that, linear model considers absorption/partitioning and adsorption of pollutant onto organic matter,

Freundlich isotherm considers the heterogeneity of the adsorbent and does not limit the amount adsorbed to the monolayer.

### 3.9. Evaluation of the gross calorific value

The spent waste biomass after biosorption treatment process represents a new kind of waste problem, so the evaluation of the gross calorific value of the SWSB before and two weeks after biosorption of diesel oil and kerosene was done as an attempt to be applied as a renewable solid biofuel. The calorific value of SWSB recorded  $\approx 21$ , 32.91, and 33.61 MJ/kg, for SWSB before and after biosorption of diesel oil and kerosene, respectively. This proves the persistence of the adsorbed petroleum hydrocarbons on the adsorbent and the improvement of the calorific value of SWSB by adsorption process, which can be used as a renewable solid biofuel in boilers or cement industries. Similar observation was reported by Brandao et al. [6] for biosorption of gasoline on natural sugarcane bagasse.

## 4. Conclusion

SWSB biomass from bioethanol production process, which is one of the major organic agricultural wastes in Egypt, proved to be a promising low-cost biosorbents for removal of different petroleum hydrocarbons products from water over a wide range of initial pollutant concentration, pH, salinity, and temperature. Based on the applied experimental conditions, the values of the adsorption capacity ranged between 40–260 mg/g for diesel oil and 44–270 mg/g for kerosene, which shows that, the SWSB has a great potential to remove petroleum hydrocarbons products from aqueous solutions. The SWSB after biosorption process expressed good calorific value which encourages its application as a renewable solid biofuel. This study proves that agricultural wastes would offer a four-fact solution: economic, energy, environmental, and waste management.

## References

- [1] V. Rajakovic, G. Aleksic, M. Radetic, L. Rajakovic, Efficiency of oil removal from real wastewater with different sorbent materials, *J. Hazard. Mater.* 143 (2007) 494–499.
- [2] S. Ibrahim, S. Wang, H.M. Ang, Removal of emulsified oil from oily wastewater using agricultural waste barley straw, *Biochem. Eng. J.* 49 (2010) 78–83.
- [3] J.M. Benito, G. Rios, C. Pasoz, J. Coca, Methods for the separation of emulsified oil from water: A state-of-the-art review, *Trends Chem. Eng.* 4 (1998) 203–231.
- [4] Y.B. Zhou, X.Y. Tang, X.M. Hu, S. Fritschi, J. Lu, Emulsified oily wastewater treatment using a

- hybrid-modified resin and activated system, Sep. Purif. Technol. 63 (2008) 400–406.
- [5] P.K. Mishra, S. Mukherji, Biosorption of diesel and lubricating oil on algal biomass, Biotechnology 2 (2012) 301–310.
- [6] P.C. Brandao, T.C. Souza, C.A. Ferreira, C.E. Hori, L.L. Romanielo, Removal of petroleum hydrocarbons from aqueous solution using sugarcane bagasse as adsorbent, J. Hazard. Mater. 175 (2010) 1106–1112.
- [7] K. Kenes, O. Yerdos, M. Zulkair, D. Yerlan, Study on effectiveness of thermally treated rice husks for petroleum adsorption, J. Non-Cryst. Solids 358 (2012) 2964–2969.
- [8] N.Sh. El-Gendy, H.R. Madian, Ligno-Cellulosic Biomass for Production of Bio-Energy in Egypt, Lambert Academic Publishing, Saarbrücken, Germany, 2013.
- [9] N.K. Amin, Removal of reactive dye from aqueous solutions by adsorption onto activated carbons prepared from sugarcane bagasse pith, Desalination 223 (2008) 152–161.
- [10] L.V.A. Gurgel, R.P. Freitas, L.F. Gil, Adsorption of Cu(II), Cd(II), and Pd(II) from aqueous single metal solutions by sugarcane bagasse and mercerized sugarcane bagasse chemically modified with succinic anhydride, Carbohydr. Polym. 74 (2008) 22–929.
- [11] B.H. Hameed, A.A. Rahman, Removal of phenol from aqueous solutions by adsorption onto activated carbon prepared from biomass material, J. Hazard. Mater. 160 (2008) 576–581.
- [12] R. Amer, N.Sh. El-Gendy, T. Taha, S. Farag, Y. Adel Fattah, Biodegradation of crude oil and its kinetics using indigenous bacterial consortium isolated from contaminated area in Egyptian Mediterranean ecosystem, JÖKULL J. 64(4) (2014) 42–52.
- [13] M.M. El-Tokhi, Y.M. Moustafa, Heavy metals and petroleum hydrocarbons contamination of bottom sediment of ElSukhna area, Gulf of Suez, Egypt, Petrol. Sci. Technol. 19 (2001) 481–494.
- [14] ASTM Standards D2015-96, Standard test method for gross calorific value of coal and coke by the adiabatic bomb calorimeter, In: Annual Book of ASTM Standards, Section 5, Vol. 05.05. West Conshohocken, PA, American Society for Testing and Materials, 1998, pp. 239–247.
- [15] D. Lin, B. Pan, L. Zhu, B. Xing, Characterization and phenanthrene sorption of tea leaf powders, J. Agric. Food Chem. 55 (2007) 5718–5724.
- [16] B. Chen, E.J. Johnson, B. Chefetz, L. Zhu, B. Xing, Sorption of polar and nonpolar aromatic organic contaminants by plant cuticular materials: The role of polarity and accessibility, Environ. Sci. Technol. 39 (2005) 6138–6146.
- [17] N. Feng, X. Guo, S. Liang, Adsorption study of Cu(II) by chemically modified orange peels, J. Hazard. Mater. 164(2–3) (2009) 1286–1292.
- [18] B. Chen, Y. Wang, D. Hu, Biosorption and biodegradation of polycyclic aromatic hydrocarbons in aqueous solution by a consortium of white-rot fungi, J. Hazard. Mater. 179 (2010) 845–851.
- [19] R. Bodirlau, C.A. Teacas, Fourier transform infrared spectroscopy and thermal analysis of lignocellulose fillers treated with organic anhydrides, Rom. J. Phys. 54 (2009) 93–104.
- [20] V.C. Srivastava, I.D. Mall, I.M. Mishra, Characterization of mesoporous rice husk ash (RHA) and adsorption kinetics of metal ions from aqueous solution onto RHA, J. Hazard. Mater. 134(1–3) (2006) 257–267.
- [21] C.G. Rocha, D.A.M. Zaia, R.V. da Silva Alfaya, A.A. da Silva Alfaya, Use of rice straw as biosorbent for removal of Cu(II), Zn(II), Cd(II) and Hg(II) ions in industrial effluents, J. Hazard. Mater. 166 (2009) 383–388.
- [22] S.L. Wang, Y.M. Tzou, Y.H. Lu, G. Sheng, Removal of 3-chlorophenol from water using rice-straw-based carbon, J. Hazard. Mater. 147 (2007) 313–318.
- [23] R. Crisafully, M.A. Milhome, R.M. Cavalcante, E.R. Silveira, D.D. Keukeleire, R.F. Nascimento, Removal of some polycyclic aromatic hydrocarbons from petrochemical wastewater using low-cost adsorbents of natural origin, Bioresour. Technol. 99 (2008) 4515–4519.
- [24] J.Y. Farah, N.Sh. El-Gendy, L.A. Farahat, Biosorption of Astrazone Blue basic dye from an aqueous solution using dried biomass of Baker's yeast as a low cost biosorbent, J. Hazard. Mater. 148 (2007) 402–408.
- [25] A.M. Djerdjjev, J.K. Beattie, Electroacoustic and ultrasonic attenuation measurements of droplet size and  $\xi$ -potential of alkane-in-water emulsions: Effects of oil solubility and composition, Phys. Chem. 10 (2008) 4843–4852.
- [26] W.J. Weber, F. Digiano, Process Dynamics in Environmental Systems, Wiley Interscience, New Jersey, 1996.
- [27] M. Dogan, M. Alkan, A. Turkyilmaz, Y. Özdemir, Kinetics and mechanism of removal of methylene blue by adsorption onto perlite, J. Hazard. Mater. B 109 (2004) 141–148.
- [28] V.S. Mane, I.D. Mall, V.C. Srivastava, Kinetic and equilibrium isotherm studies for the adsorption removal of brilliant Green dye from aqueous solutions by rice husk ash, J. Environ. Manage. 84 (2007) 390–400.
- [29] S. Lagergren, About the theory of so-called adsorption of soluble substances, Kungliga Svenska Vetenskapssakademien, R. Swedish Acad. Sci. 24 (1898) 1–3.
- [30] Y.S. Ho, G. McKay, Pseudo-second-order model for sorption processes, Process Biochem. 34 (1999) 451–465.
- [31] V.K. Gupta, I. Ali, Suhas, D. Mohan, Equilibrium uptake and sorption dynamics for the removal of a basic dye (Basic Red) using low-cost adsorbents, J. Colloid Interface Sci. 265(2) (2003) 257–264.
- [32] A. Ozer, G. Akkaya, M. Turabik, The removal of Acid Red 274 from wastewater: Combined biosorption and bio-coagulation with *Spirogyra rhizopus*, Dyes Pigm. 71 (2006) 83–89.
- [33] H.J. El-Aila, K.M. El-Sousy, K.A. Hartany, Kinetics, equilibrium and isotherm of the adsorption of cyanide by MDFSD, Arabian J. Chem. (2011) (article in press).
- [34] B.D. Bohel, B. Ganguly, A. Madhuran, D. Deshpande, J. Joshi, Biosorption of Methyl Violet, basic Fuchsin and their mixture using dead fungal biomass, Curr. Sci. 86 (2004) 1641–1645.
- [35] C.F. Iscen, I. Kiran, S. Ihan, Biosorption of Reactive Black 5 dye by *Penicillium restrictum*: The kinetic study, J. Hazard. Mater. 143(1–2) (2007) 335–340.
- [36] P.S. Malik, Dye removal from wastewater using activated carbon developed from sawdust: Adsorption equilibrium and kinetics, J. Hazard. Mater. 113 (2004) 81–88.

- [37] X. Chen, J. Yu, Z.H. Zhang, C. Lu, Study on structure and thermal stability properties of cellulose fibers from rice straw, *J. Carbohydr. Polym.* 85 (2011) 245–250.
- [38] I. Langmuir, The constitution and fundamental properties of solids and liquids, *J. Am. Chem. Soc.* 38(11) (1916) 2221–2295.
- [39] S.J. Allen, G. McKay, J.F. Poter, Adsorption isotherm models for basic dye adsorption by peat in single and binary component systems, *J. Colloid. Interf. Sci.* 280 (2004) 332–333.
- [40] T.W. Weber, R.K. Chakravorti, Pore and solid diffusion model for fixed bed absorbers, *AIChE J.* 20(2) (1974) 2228.
- [41] H.M.F. Freundlich, Über die adsorption in lösungen, *Zeitschrift für Physikalische Chemie J. Phys. Chem.* 57 (1906) 385–470.
- [42] R.E. Treybal, *Mass Transfer Operation*, third ed., McGraw-Hill Book Company, New York, NY, 1980.
- [43] M.J. Temkin, V. Pyzhev, Kinetics of ammonia synthesis on promoted iron catalysis, *Acta Physiochim. URSS* 12 (1940) 327–356.
- [44] Y. Liu, Y.J. Liu, Biosorption isotherms, kinetics and thermodynamics, *Sep. Purif. Technol.* 61 (2008) 229–242.
- [45] J. Anwar, U. Shafique, W. Zaman, M. Salman, A. Dar, Sh. Anwar, Removal of Pb(II) and Cd(II) from water by adsorption on peels of banana, *Bioresour. Technol.* 101 (2010) 1752–1755.
- [46] H.K. Boparai, M. Joseph, D.M. O'Carroll, Kinetics and thermodynamics of cadmium ion removal by adsorption onto nano zerovalent iron particles, *J. Hazard. Mater.* 186 (2011) 458–465.
- [47] J.Y. Farah, N.Sh. El-Gendy, Performance, kinetics and equilibrium in biosorption of anionic dye Acid Red 14 by the waste biomass of *Saccharomyces cerevisiae* as a low-cost biosorbent, *Turkish J. Eng. Env. Sci.* 37 (2013) 146–161.